medRxiv preprint doi: https://doi.org/10.1101/2020.04.08.20058842; this version posted May 4, 2020. The copyright holder for this preprint (which was not certified by peer review) is the author/funder, who has granted medRxiv a license to display the preprint in perpetuity. It is made available under a CC-BY-NC-ND 4.0 International license .

The Epidemiological Implications of Incarceration Dynamics in Jails for Community, Corrections Officer, and Incarcerated Population Risks from COVID-19

Eric Lofgren[1◑], Kristian Lum[2◑], Aaron Horowitz[3], Brooke Madubuonwu[3], Kellen Myers[4], Nina H. Fefferman[5,6*]

1 Paul G. Allen School for Global Animal Health, Washington State University, Pullman, WA USA
2 Department of Computer and Information Science, University of Pennsylvania, Philadelphia, PA, USA
3 ACLU Analytics, American Civil Liberties Union, New York, NY USA
4 Department of Mathematics, Tusculum University, Greeneville, TN, USA
5 Department of Mathematics, University of Tennessee, Knoxville, TN, USA
6 Department of Ecology and Evolutionary Biology, University of Tennessee, Knoxville, TN, USA

◑These authors contributed equally to this work.
* nfefferm@utk.edu

Abstract

COVID-19 challenges the daily function of nearly every institution of society. In response to these challenges, mathematical models allow us to combine a mechanistic understanding of disease spread in general with the best information currently available on the particulars of this disease to analyze the costs and benefits of any mitigative action. We here provide one such mathematical model to explore the epidemiological consequences of allowing standard intake and unaltered within-jail operational dynamics to be maintained during the ongoing COVID-19 pandemic, and contrast this with proposed interventions to reduce the burden of negative health outcomes. In this way, we provide estimates of the infection risks, and likely loss of life, that arise from current incarceration practices. We provide estimates for in-custody deaths and show how the within-jail dynamics lead to spill-over risks, not only affecting the incarcerated people, but increasing the exposure, infection, and death rates for both corrections officers with whom they interact within the jail system, and the broader community beyond the justice system. We show that, given a typical jail-community dynamic, operating in a business as usual way will result in significant and rapid loss of life. Large scale reductions in arrest and speeding of releases are likely to save the lives of incarcerated people, jail staff, and the community at large.

Introduction

As the COVID-19 pandemic sweeps the globe, one of the critical functions of epidemiology is to consider how society can transform current practice to increase the health and safety of the public. Given the widespread risk of infection and the high case fatality rates, especially in older or medically compromised populations, the most effective strategies to reduce the impact of the disease may require that we be willing to

NOTE: This preprint reports new research that has not been certified by peer review and should not be used to guide clinical practice.

medRxiv preprint doi: https://doi.org/10.1101/2020.04.08.20058842; this version posted May 4, 2020. The copyright holder for this preprint (which was not certified by peer review) is the author/funder, who has granted medRxiv a license to display the preprint in perpetuity. It is made available under a CC-BY-NC-ND 4.0 International license .

consider structural reforms to our institutions to promote an overall greater good. To these ends, we have already seen systemic shifts in institutional practices that would be unthinkable under normal conditions: shelter-in-place orders closing businesses and restricting freedom of individual movement [1], school closures to limit transmission compromising the ongoing education of children [2], etc. Another clearly important institution that affects a substantial portion of the public directly [3] and an even greater portion indirectly [4–7], is our criminal legal system. The currently unfolding public health crisis makes clear the urgent need for rigorous analyses of the impact of maintaining current practices within these institutions, including both the costs to incarcerated people and their families as well as the costs to the community at large. We therefore explore the epidemiological costs associated with our current system's functions as a necessary part of the policy conversation that must ensue to decide whether or not they should be maintained or altered in response to a growing global crisis.

Analyzing incarcerated populations poses a unique epidemiological problem for several reasons. The population experiences high rates of movement and turnover [8, 9]. Incarcerated people are responsible for purchasing their own hygiene products with limited resources [10, 11]. It is difficult or impossible for incarcerated people to practice CDC recommendations such as social distancing [12]. The incarcerated population has a higher expected rate of existing health conditions than the community from which they come [13–15]. Jails are dependent completely on a workforce that moves in and out of the jail and the community including vendors, lawyers, corrections officers, medical staff, etc. And, there is strong evidence that incarceration itself has profound adverse effects on the health of incarcerated people [16–18]. These descriptors make jails highly likely not only to place detained people at increased risk of infection and resulting severe outcomes, but also to function as a driver for increased infectivity, adversely impacting attempts to contain and mitigate disease spread in the broader communities in which jails are located. To study the dynamics of this system and provide quantitative metrics for risk to incarcerated populations and the populations with which incarcerated people necessarily interact, we construct and tailor a epidemiological model of COVID-19 transmission, and then use that model to consider how some possible reforms to the system (i.e. reduction in arrest intake, increased rates of returning incarcerated people to their homes, and improvement of conditions within the jails) will alter these baseline risks.

Model/Methods

Transmission Model

We begin by tailoring a standard SEIR model to the specific dynamics of COVID-19. We first split our total population into four categories of risk: Children under 18 (denoted with the subscript K), Low-risk adults (denoted with the subscript L), High-risk adults (denoted with the subscript H), and Elderly adults (denoted with the subscript E). We also designate a separate population category for jail staff, O (note: while O was the selected notation, it is meant to capture all staff working at the jail, not only the corrections officers). These populations are then assigned into disease-related health status compartments: Susceptible (S), Exposed (in which individuals are presymptomatic, but do already produce low levels of infection transmission to others, E), Infected (in which individuals are both symptomatic themselves and fully infectious to others, I), Medically Treated (those infectious individuals whose disease severity and healthcare access results in removal from the population into a medical care facility that prevents any further transmission of infection back into the population, M), and

medRxiv preprint doi: https://doi.org/10.1101/2020.04.08.20058842; this version posted May 4, 2020. The copyright holder for this preprint (which was not certified by peer review) is the author/funder, who has granted medRxiv a license to display the preprint in perpetuity. It is made available under a CC-BY-NC-ND 4.0 International license .

Removed (those who have either recovered from the infection and are now immune or those who have died, R). We also allow for the possibility that an Infected person with sufficient disease severity to warrant medical treatment is unable to obtain care, and designate rates associated with this case, as designated by the subscript U. For clarity of the results, we do not consider death from any non-COVID-19 cause; this is done to highlight the COVID-19-specific dynamics. Additionally, as a simplifying assumption due to their low rates of both infections and complications, we do not model hospitalizations or deaths in children. Similarly, once hospitalized, patients are assumed not to spread COVID-19 further, as additionally modeling the impact of healthcare-associated COVID-19 cases is well beyond the scope of this model. Lastly, we split our population into segments depending on the subsection of the community or jail system in which they are currently functioning: the community at large, C, the processing system for the jail, P, the court system T, and the jail system, J.

A schematic for this model can be seen in Fig. 1, and the differential equations comprising the model are in SI Appendix 1. The model was implemented in R 3.6.3 using the deSolve package, with the visualization of results primarily using ggplot2. Statistical analysis of one parameter (see below) was done using the flexsurv package. The code and data used in this analysis is available at https://www.github.com/epimodels/COVID19-Jails. As this study used only publicly available data and does not involve human subjects, IRB approval was not required.

medRxiv preprint doi: https://doi.org/10.1101/2020.04.08.20058842; this version posted May 4, 2020. The copyright holder for this preprint (which was not certified by peer review) is the author/funder, who has granted medRxiv a license to display the preprint in perpetuity. It is made available under a CC-BY-NC-ND 4.0 International license .

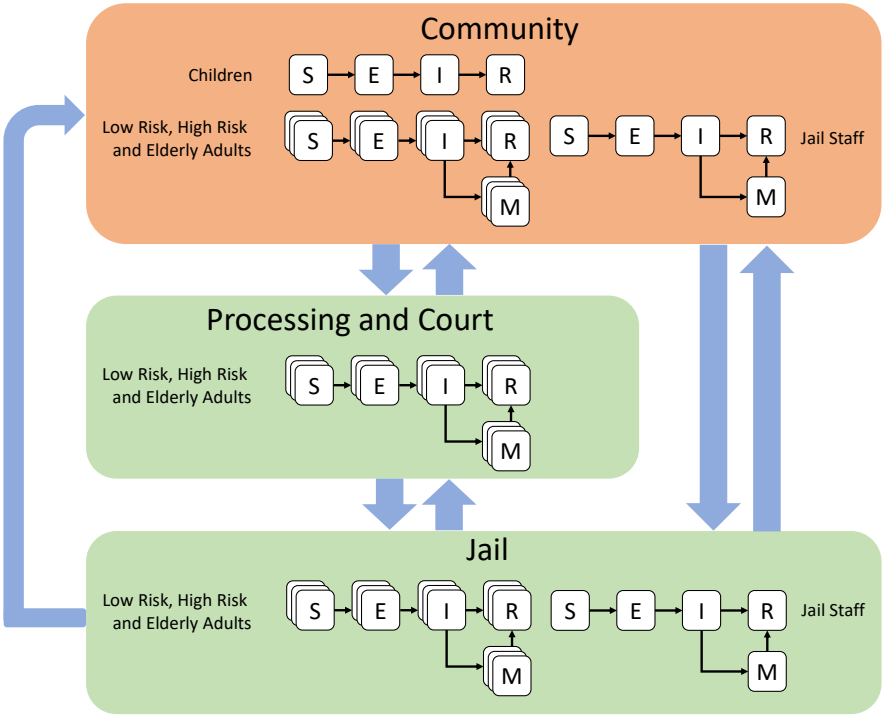

Fig 1. Schematic for a mathematical model of COVID-19 in a linked urban community - jail system. The population is represented in one of five possible compartments: Suseptible (S), Exposed (E), Infected (I), Needing Medical Care (M) and Recovered/Removed (R). Additionally, the population is divided into five distinct sub-populations: Children under 18 years of age, Elderly Adults over 65 years of age, Low Risk Adults between 18 and 65, High Risk Adults between 18 and 65 and Jail Staff (assumed to be between 18 and 65 years of age). Arrested adults move between the Community, Processing and the Court System and Jail, while Jail Staff move between the Community and Jail. Children are assumed not to be eligible for arrest.

Population Movement Into, Within, and Out Of the Jail System

Our model captures movement between the community (denoted with superscript, C), processing (P),jail (denoted with superscript, J), and court appointments (denoted with T for trial, though this is meant to encompass all court appointments). It assumes staff move only between the community and jail; they are not arrested in our model. We base the parameters of movement into, within, and out of the jail on Allegheny County, Pennsylvania, where detailed data on the jail population and facilities are available, including an automatically updating dashboard giving statistics for the jail population.[1] In Allegheny County, the population at large is approximately 1.2 million people. The size of the jail population hovers around 2,500. We use these population figures to initialize our model.

In our model, individuals in the community are arrested at a rate of approximately 100 people per day.[2] Arrested individuals are brought to processing. From processing, individuals can either be released back into the community (60%) or taken to jail (40%)[3]. This results in an in-flow to the jail of approximately 40 individuals per day, which is

[1] https://perma.cc/93RG-4WZ8
[2] https://perma.cc/9DSP-9CTY
[3] https://perma.cc/93RG-4WZ8

medRxiv preprint doi: https://doi.org/10.1101/2020.04.08.20058842; this version posted May 4, 2020. The copyright holder for this preprint (which was not certified by peer review) is the author/funder, who has granted medRxiv a license to display the preprint in perpetuity. It is made available under a CC-BY-NC-ND 4.0 International license .

consistent with Allegheny County's reporting. While in jail, individuals transition back and forth between the jail and court appointments. The number of movements between jail and court appointments is described as "well over 100" on the jail's website. We assume movement of approximately 150 people per day between the jail and court. For each court appointment, we assume individuals spend half a day on average at the court facility. Importantly, we also assume that there is mixing in the court facility between those who are there for processing after arrest and those that are present there for court appointments. From the jail, individuals are released back into the community at a rate that is consistent with the reported 62 day average length of stay. One limitation of our model is that we do not account for post-jail destinations that are not the community, i.e. we do not model people moving from jail to prison. According to [19], the yearly number of admissions to prison is about 600,000 while the yearly number of admissions to jail is around 10.6 million. So, assuming that all prison admissions first had one jail admissions, around 95% of all jail admissions do not go on to prison; they are released back into the community as in our model. Thus, we expect that the omission of prison from our model does not substantially impact the overall findings.

An online database of public employees salaries in Allegheny County shows a population of 384 people whose job title is corrections officer, whose job location is the jail, and who are listed as active. Although this is certainly an underestimate of the total number of the jail's staff, which includes other types of employees, we think this is a useful approximation to the total number of staff. We use this figure as the number of staff members moving between community and jail. Staff transition between community and jail at a rate that assumes 8 hour shift lengths in the jail per day with the remaining 16 hours per day spent in the community.

Estimation Population Mixing and Contact Rates

We estimate parameters that describe the relative rate of transmission between each of the community categories: Children, Low-risk adults, High-risk adults, and Elderly adults from other studies. We use β_{qr}^{C*} to denote the relative rate of transmission to category q from category r. We estimate this as

$$\beta_{qr}^{C*} = m_{qr} c_q p_q^{-1} t_q.$$

m_{qr} is the number of times a person in category q is in contact with a person in category r. We use the category-category contact rates given in [20]. c_q is the proportion of COVID-19 cases that occurred for people in category q and p_q is the proportion of the total population in category q. The ratio of these two terms, $c_q p_q^{-1}$, is meant to capture the relative proclivity for people in group q to be infected by the virus. We use case counts and population information for South Korea as reported by Statista.[4]. t_i is the number of daily contacts for individuals in category q, as reported in [21]. The β^*s are normalized such that the Child-Child transmission is equal to one. The resulting values of β_*^C is shown in Table 1.

	child	adult	elderly
child	1.00	0.51	0.08
adult	0.57	2.43	1.05
elderly	0.02	0.30	0.49

Table 1. Relative transmission rates of COVID-19 from an individual per row to an individual per column, scaled so that the Child-Child rate is one.

[4]COVID-19 case proportions: https://www.statista.com/statistics/1102730/south-korea-coronavirus-cases-by-age/

medRxiv preprint doi: https://doi.org/10.1101/2020.04.08.20058842; this version posted May 4, 2020. The copyright holder for this preprint (which was not certified by peer review) is the author/funder, who has granted medRxiv a license to display the preprint in perpetuity. It is made available under a CC-BY-NC-ND 4.0 International license .

Within the jail and processing, we assume that mixing patterns are not category-dependent. We set $\beta^{J*} = \beta^{J*}_{qr} = \beta^{C*}_{LL} c_j$, $\beta^{P*} = \beta^{P*}_{qr} = \beta^{C*}_{LL} c_p$, and $\beta^{T*} = \beta^{T*}_{qr} = \beta^{C*}_{LL} c_t$, where β^{C*}_{LL} is the low risk adult to low risk adult base transmission rate in the community and c_j, c_p, and c_t are factors that denotes how times more contacts per day a person in jail or processing, respectively, has than a person in the community. We set these values to be $c_j = 3$ and $c_p = c_t = 6$, corresponding to an assumption of three and six times more contact in jail and processing/trial, respectively, than take place in the community.

The β^*s are defined on an arbitrary scale. To get simulations that resemble the real spread of the virus, we calibrated the model. We set $\beta^C_{qr} = \frac{c_0 \beta^{C*}_{qr}}{n_c}$, $\beta^J = \frac{c_0 \beta^{J*}}{n_j}$, $\beta^T = \frac{c_0 \beta^{T*}}{n_t}$, and $\beta^P = \frac{c_0 \beta^{P*}}{n_p}$, where $n_c = 1,200,000$, $n_j = 2,600$, $n_t = 250$, and $n_p = 250$ are the size of the population in the community, jail, and processing, respectively, and c_0 is a calibration parameter. Scaling each of the β terms in the model by the population sizes amounts to the assumption that transmission is contact-based. This assumption leads to conservative estimates of the speed of the spread in the jail system relative to a fomite-based transmission model. To calibrate the model, we then find a c_0 such that approximately 80% of the population is ultimately infected by the time the spread dies out in our model. We selected an 80% final infection rate for consistency with predictions of the spread of COVID-19 under the assumption of no mitigation measures in place from an influential micro-simulation model [22].

Estimation of Other Model Parameters

Parameters concerning the natural history of COVID-19, patient progression, etc. were primarily obtained from existing estimates in the modeling literature, where possible using estimates from as close to the modeled catchment area as possible (i.e. CHIME from UPenn Medicine, https://penn-chime.phl.io/). Citations for specific parameter values may be found in Table 2.

In one case, $\hat{\gamma}$, or the asymptomatic period^{-1}, the original source reported that their estimate was likely an underestimation due to censoring. However, given that the authors provided the data within their manuscript [23], the data was re-estimated to account for censoring using a parametric survival model assuming an exponential distribution (the distribution typically implied by the uniform hazard of transitioning from one compartment to another within a compartmental model). The fit for this exponential model may be found in SI Appendix 2.

Modeled Scenarios and Interventions

We represented the effects of several policy interventions or failures as changes to various parameters in this model. We consider four categories of scenarios that could vary the rate of spread: in addition to modeling shelter-in-place (reduced mixing) conditions in the community, we modeled scenarios related to reductions in arrest rates, increases in release rates, and changes to within-jail conditions. These scenarios are detailed below in Table 3. Most scenarios are additive; that is, all arrest reduction interventions assume a baseline scenario of shelter-in-place in the community. The scenarios involving faster release of individuals in jail all assume both shelter-in-place in the community, and were each run under each of the "Arrest Reduction" scenarios to determine the cumulative effects of arrest reduction, increased release rates, and community shelter-in-place conditions. The mixing reduction scenario in the jail assumes shelter-in-place in the community as well as a 25% reduction in arrests (equivalent to the "Bail Eligible" Arrest Reduction scenario), as it is unlikely that jails will be able to effectively reduce contact rates without reducing their average daily population. Finally,

medRxiv preprint doi: https://doi.org/10.1101/2020.04.08.20058842; this version posted May 4, 2020. The copyright holder for this preprint (which was not certified by peer review) is the author/funder, who has granted medRxiv a license to display the preprint in perpetuity. It is made available under a CC-BY-NC-ND 4.0 International license .

	Parameter	Value	**Description**
1	σ	0.50	Percent reduction in transmission during asymptomatic period (compared to symptomatic) [24]
2	γ^{-1}	5.1 days	Incubation Period [25]
3	$\hat{\gamma}^{-1}$	6.7 days	Asymptomatic Period [23]
4	δ^{-1}	10 days	Symptomatic Period [24]
5	$\delta^{-1}_{Discharge}$	9 days	Hospitalization Length of Stay (Discharged Alive) [26][5]
6	δ^{-1}_{Death}	4.2 days	Hospitalization Length of Stay (Discharge Dead) [26]
7	δ^{-1}_{DeathU}	4.2 days	Time to Death for Unhospitalized Critical Cases
8	ω_L	5.9 days$^{-1} * 0.0625$	Time from Symptom Onset to Hospitalization * Probability of Needing Hospitalization (low risk) [26, 27]
9	ω_H	5.9 days$^{-1} * 0.118$	Time from Symptom Onset to Hospitalization * Probability of Needing Hospitalization (high risk) [26, 27]
10	ν	95%	Hospitalized Case Survival Rate (low risk) [28]
11	ν_H	66.6%	Hospitalized Case Survival Rate (high risk) [28]
12	ν_U	0.0%	Unhospitalized Critical Case Survival Rate (low risk)
13	ν_{UH}	0.0%	Unhospitalized Critical Case Survival Rate (high risk)
14	α_L	3.57e-06	Per Capita Hourly Arrest Rate (low risk). Equates to 60 arrests per day.
15	α_E	7.35e-06	Per Capita Hourly Arrest Rate (elderly). Equates to 1 arrest per day.
16	α_H	1.11e-03	Per Capita Hourly Arrest Rate (high risk). Equates to 40 arrests per day.
17	ψ_C	12 hours$^{-1} * 0.60$	Processing Time from Arrest to Returning to Community * Probability of Release After Arrest
18	ψ_J	12 hours$^{-1} * 0.40$	Processing Time from Arrest to Jail * Probability of Jail After Arrest
19	κ	2.60e-03	Per Capita Hourly Probability of Scheduled Court Appearance
20	τ	12 hours	Time from Scheduled Court Appearance to Return to Jail
21	ρ^{-1}	62 days	Length of Stay in Jail [6]
22	μ_C^{-1}	8 hours	Shift Length for Jail Staff
23	μ_J^{-1}	16 hours	Time Spent in the Community for Jail Staff
24	ζ	1.00	Probability an Incarcerated Person Needing Treatment Will Receive It
25	pop	1.22 million people	Population of Jail Catchment Area

Table 2. Parameter values, meanings and sources for a community-jail transmission model of COVID-19.

medRxiv preprint doi: https://doi.org/10.1101/2020.04.08.20058842; this version posted May 4, 2020. The copyright holder for this preprint (which was not certified by peer review) is the author/funder, who has granted medRxiv a license to display the preprint in perpetuity. It is made available under a CC-BY-NC-ND 4.0 International license .

in the reduced detection scenario, we assume shelter-in-place, but vary the likelihood that serious cases of COVID-19 is caught and treated in a timely manner.

Below, vulnerable populations are defined as individuals over the age of 65 or at increased risk of complications form COVID-19 due to other co-morbidities. We estimate that 40% of the jail population is vulnerable by this definition, according to information from the Bureau of Justice Statistics [29]. We estimate that around 25% of those arrested are bail eligible, based on information from Allegheny county that cash bail was used in 28% of cases between February and June of 2019 [30].

Scenario Name	**Parameters**	**Multiplier of Baseline**	**Scenario Description**
Shelter in Place	β_*^C	0.625	Effective contact rate in the community is reduced by a factor of 1/1.6.
Arrest Reduction			
Bail Eligible	α_L, α_H, α_E	0.75	Divert all bail-eligible arrests (estimated at 25% of all arrests)
Vulnerable Only	α_H, α_E	0.10	Divert arrests of 90% of vulnerable populations. [9]
Low Level	α_L, α_H, α_E	0.17	Divert all low-level arrests (estimated at 83% of arrests).
Arrest Fewer People	α_L, α_H, α_E	0.10	Divert 90% of current arrests.
Faster Release			
Increase Release Speed	ρ^{-1}	2	2x rate of release from jail
Vulnerable Only	ρ_H^{-1}	2	2x rate of release for vulnerable only
In-Jail Scenarios			
Mixing Reduction	β_T, β_P, β_J	0.625	Reduction of baseline contact rates in jails by the same factor as the community under shelter-in-place
Reduced Detection	ζ	0.99,0.95,0.90	Reduction in infection detection and timely hospitalization in jails by 1-ζ

Table 3. Scenarios and parameter adjustments for a number of policy-based interventions to curtail COVID-19 in jail and the community.

Results

Unsurprisingly given the epidemiological dynamics of COVID-19, absent any intervention there is a substantial outbreak in the community, causing 926,108 infections (both symptomatic and asymptomatic) as well as requiring 51,497 hospitalizations and ultimately resulting in 12,133 fatalities over the 180 days of the simulation, with the peak of infections occurring 88 days after the first infective case appeared in the population. Among those incarcerated, the outbreak is considerably more severe, causing a cumulative 4,949 cases requiring 264 hospitalizations and 79 deaths among those incarcerated, the 2500 person jail being 0.2% the size of the wider community (Fig

medRxiv preprint doi: https://doi.org/10.1101/2020.04.08.20058842; this version posted May 4, 2020. The copyright holder for this preprint (which was not certified by peer review) is the author/funder, who has granted medRxiv a license to display the preprint in perpetuity. It is made available under a CC-BY-NC-ND 4.0 International license .

2). The peak of this within-jail epidemic is also considerably earlier, with the peak of the epidemic occurring 31 days after the first infective case appeared in the community.

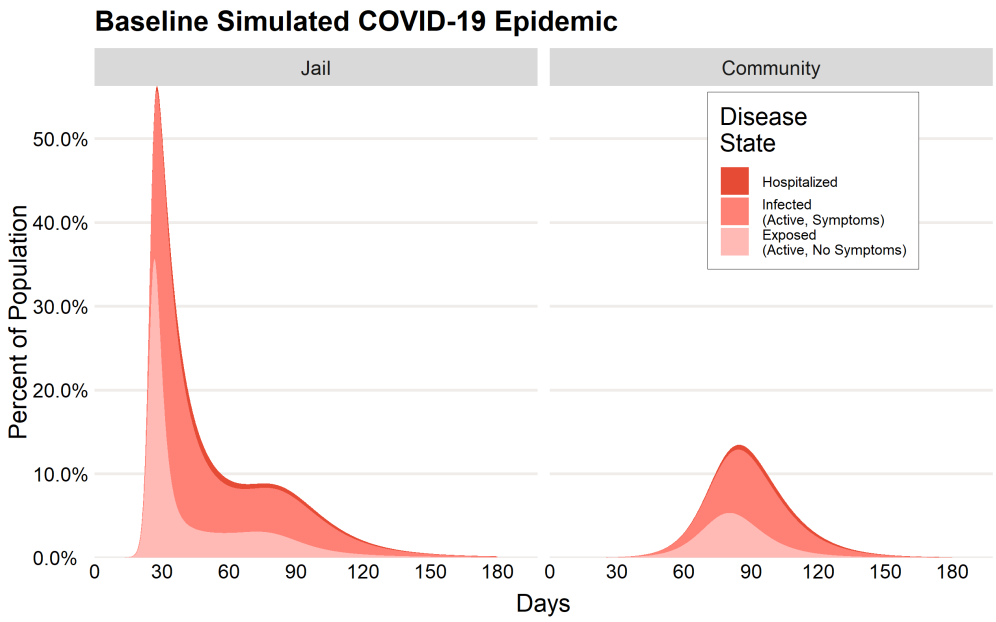

Fig 2. Epidemic curves from a simulated COVID-19 epidemic in an urban community (right) and the connected population of persons in a jail (left). The magnitude of the peak in the population in jail is much higher and shifted a full 57 days earlier.

Given the dominant approach to controlling COVID-19 in the community and the widespread calls to "flatten the curve," for the remaining results we assume the presence of a shelter-in-place order or similar social distancing intervention *only in the community* as the comparator scenario, represented as a reduction in the mixing frequency of all age groups in the community. In line with the experience of communities undergoing such distancing interventions, this decrease in overall contacts results in a substantially delayed epidemic, with 450,621 infections in the community as well as far lower burdens in terms of both hospitalizations and fatalities. In contrast, the early dynamics of the COVID-19 outbreak within the incarcerated population are identical, while in the latter half of the simulation the outbreak dynamics in the incarcerated population are markedly worse, resulting in 7421 infections after 180 days and proportionately more hospitalizations and COVID-19 related fatalities (Fig 3). Shelter-in-place orders had no discernible impact on the health outcomes of the staff of the jail.

medRxiv preprint doi: https://doi.org/10.1101/2020.04.08.20058842; this version posted May 4, 2020. The copyright holder for this preprint (which was not certified by peer review) is the author/funder, who has granted medRxiv a license to display the preprint in perpetuity. It is made available under a CC-BY-NC-ND 4.0 International license .

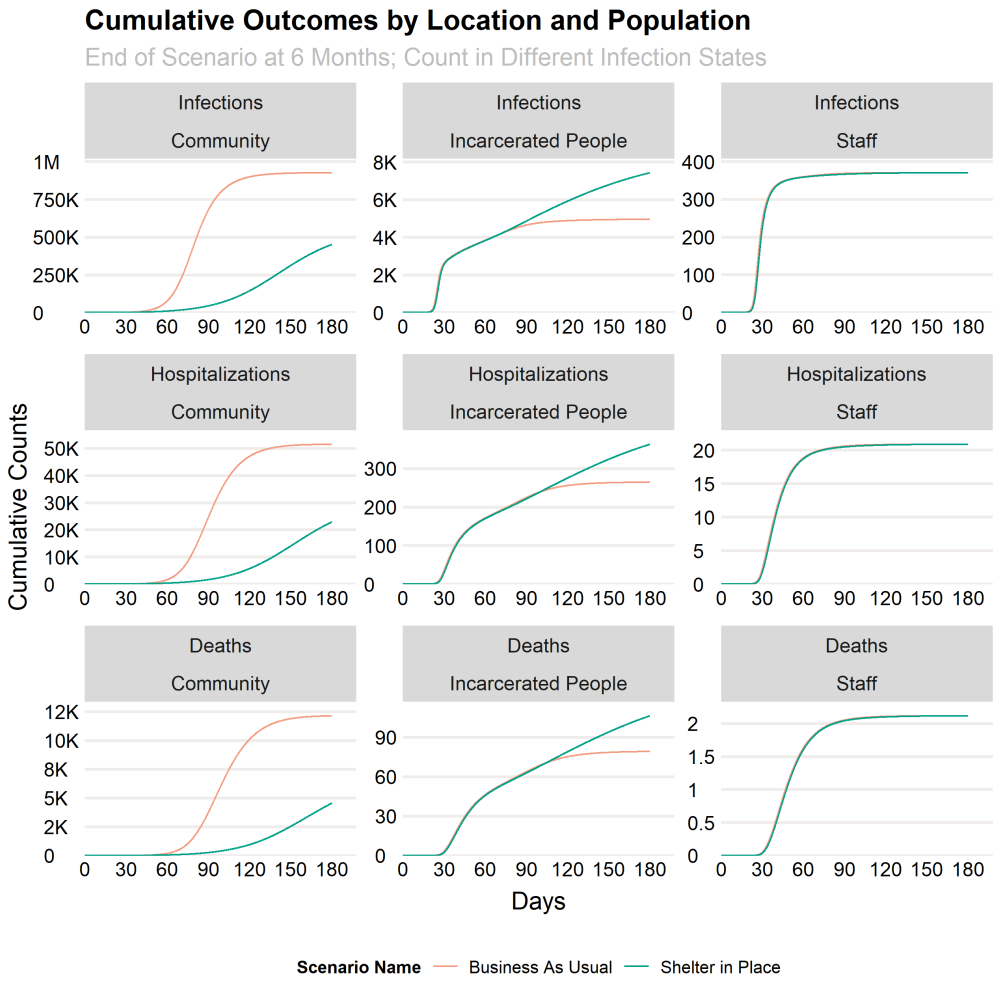

Fig 3. Cumulative infections, hospitalizations and deaths in the community (first column), among persons in jail (second column) and among jail staff (third column) for scenarios with (green) and without (orange) a shelter-in-place social distancing intervention. Such social distancing dramatically reduces the burden of infections and resulting adverse outcomes in the community, but results in a larger and more prolonged outbreak among persons in jail. Sensitivity of the number of infections to alterations in parameter values used are presented in SI Appendix 3.

All of the four considered arrest deferral scenarios had substantial impacts on the course of the epidemic in the incarcerated population, while also lessening the impact of the epidemic on the community and, to a lesser extent, the jail's staff. Discontinuing the arrest of bail-eligible individuals, which corresponds to a ≈25% reduction of admissions into the jail, resulted in a 22.9% reduction in infections in the incarcerated population, and a 3.9% reduction in infections within the community.

Broader, more sweeping arrest deferral programs resulted in correspondingly larger impacts in both the incarcerated population and the community as a whole. The discontinuation of arresting individuals for low level offenses (≈83.4% reduction) and the blanket reduction of arrests by 90% resulted in a 74.0% and 77.3% reduction in infections within the incarcerated population (with correspondingly fewer hospitalizations and deaths) respectively. These strategies also resulted in the greatest decrease in infections among staff (10.2% and 12.9%) and in the community at large

medRxiv preprint doi: https://doi.org/10.1101/2020.04.08.20058842; this version posted May 4, 2020. The copyright holder for this preprint (which was not certified by peer review) is the author/funder, who has granted medRxiv a license to display the preprint in perpetuity. It is made available under a CC-BY-NC-ND 4.0 International license .

(19.7% and 22.5%). Finally, a strategy built on deferring the arrest of individuals at high risk of developing COVID-19 related complications by 90%, tailoring the intervention to groups of epidemiological importance rather than the nature of their offense, resulted in a 28.1% decrease in infections within the incarcerated population and a 57.3% decrease in deaths among the same population.

In comparison, a strategy deferring the same number of people with no regard to their underlying risk (≈36.5%), resulted in a 7.3% decrease in overall infections within the incarcerated population, but a 60.9% increase in deaths among incarcerated persons compared to the scenario specifically targeting those at greatest risk of averse outcomes for deferred arrest (Fig 4). The deferral strategy targeting individuals for high risk outcomes caused 1.4% more infections in the community compared to the same proportionately large but broader strategy, and the decreased number of deaths among persons in jail was partially offset by this increase, with the targeted strategy resulting in a combined number of COVID-19 fatalities in both the population of persons in jail and in the community of 4208 compared to 4131 fatalities under the broader strategy.

medRxiv preprint doi: https://doi.org/10.1101/2020.04.08.20058842; this version posted May 4, 2020. The copyright holder for this preprint (which was not certified by peer review) is the author/funder, who has granted medRxiv a license to display the preprint in perpetuity. It is made available under a CC-BY-NC-ND 4.0 International license .

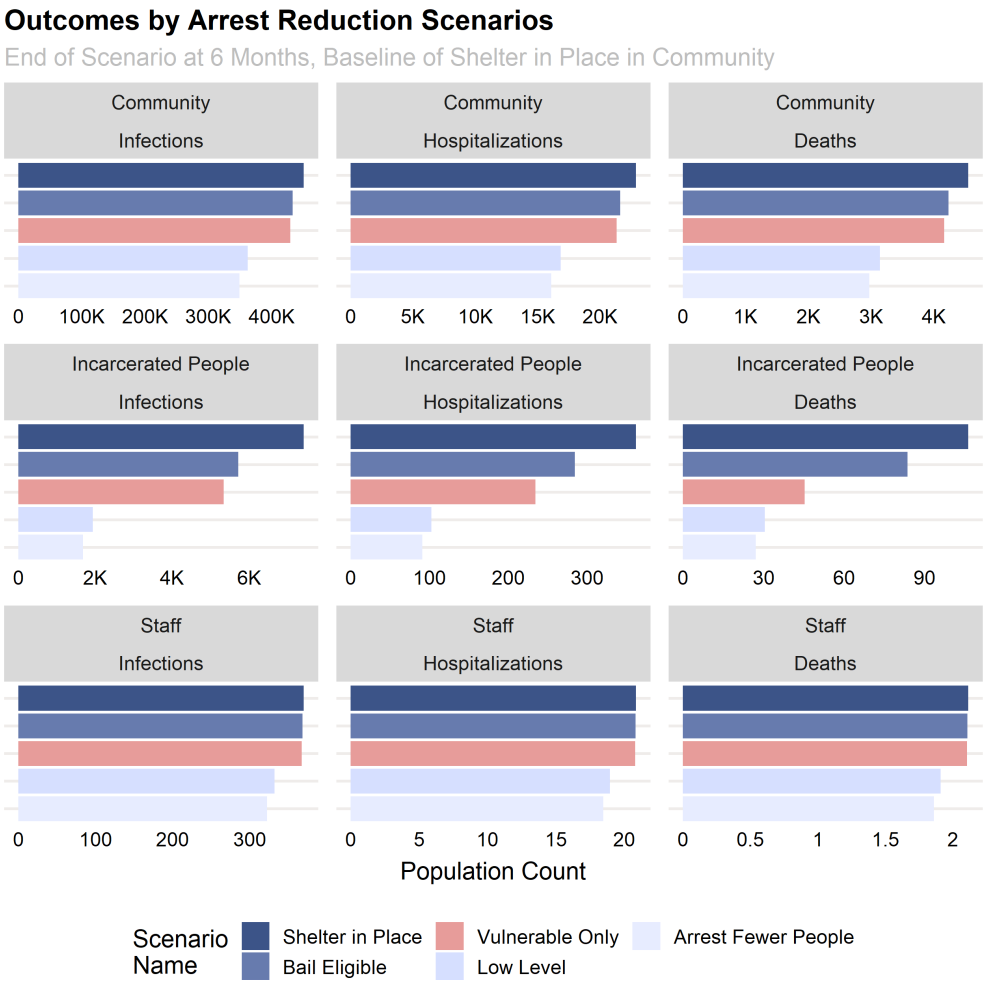

Fig 4. Cumulative infections, hospitalizations and deaths in the community (first row), among persons in jail (second row) and among jail staff (third row) for several incarceration deferment scenarios. More aggressive scenarios, such as a 90% decrease in all incarcerations or discontinuing incarceration for low level offenses result in large improvements in the epidemic within the jail, with a smaller impact among staff and the community. Deferring incarceration for people particularly at risk for adverse outcomes results in a markedly pronounced decrease in deaths among persons in jail.

Pairing increased arrest deferral with a more rapid release of persons who were already incarcerated enhanced the impact of those interventions, reducing infections, hospitalizations and deaths overall (Fig 5). The rate of decrease was less dramatic in the community and staff populations, especially at lower levels of accelerated release schedules.

medRxiv preprint doi: https://doi.org/10.1101/2020.04.08.20058842; this version posted May 4, 2020. The copyright holder for this preprint (which was not certified by peer review) is the author/funder, who has granted medRxiv a license to display the preprint in perpetuity. It is made available under a CC-BY-NC-ND 4.0 International license .

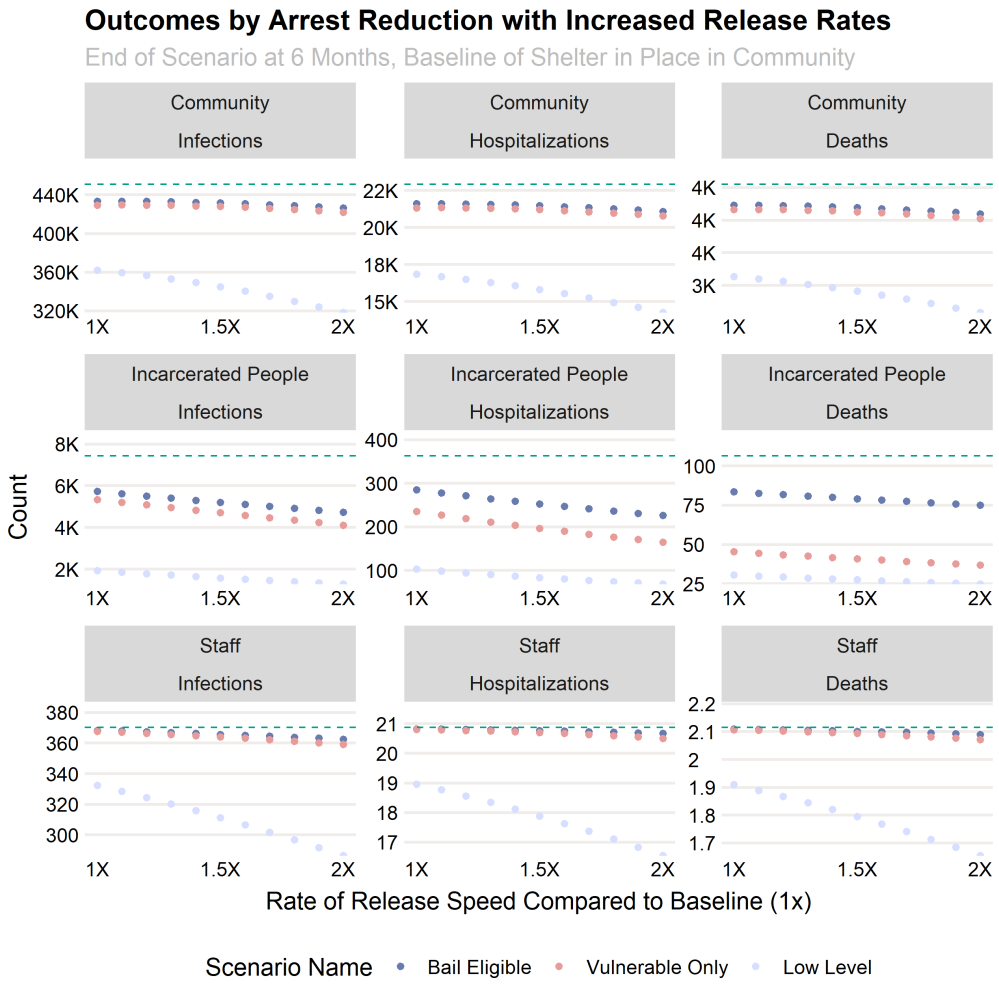

Fig 5. Cumulative infections, hospitalizations and deaths in the community (first row), among persons in jail (second row) and among jail staff (third row) for several combinations of incarceration deferment and accelerated release. Negative outcomes among persons in jail, the community as well as staff improve with faster levels of release, while the community experiences slightly worse negative outcomes.

When accompanied by the deferred arrest of bail-eligible individuals to reduce the incarcerated population, supplementary measures to reduce transmission among incarcerated persons have a marked benefit in both reducing the amplitude of the epidemic curve in incarcerated people and jail staff, as well as shifting the overall community epidemic curve later (Fig 6). These interventions may be thought of as either measures to reduce mixing — such as allowing greater space between individuals in common areas or the staggering of the use of shared facilities — or the provision of supplies such as soap and hand sanitizer that reduces the level of viral contamination of patient's hands, physical surfaces, etc. Compared to the baseline mixing rate among persons in jail, a reduction to an equivalent level of mixing as the community while sheltering in place would reduce infections in this population by 14.6% as well as delay the peak of the epidemic by approximately two weeks.

medRxiv preprint doi: https://doi.org/10.1101/2020.04.08.20058842; this version posted May 4, 2020. The copyright holder for this preprint (which was not certified by peer review) is the author/funder, who has granted medRxiv a license to display the preprint in perpetuity. It is made available under a CC-BY-NC-ND 4.0 International license .

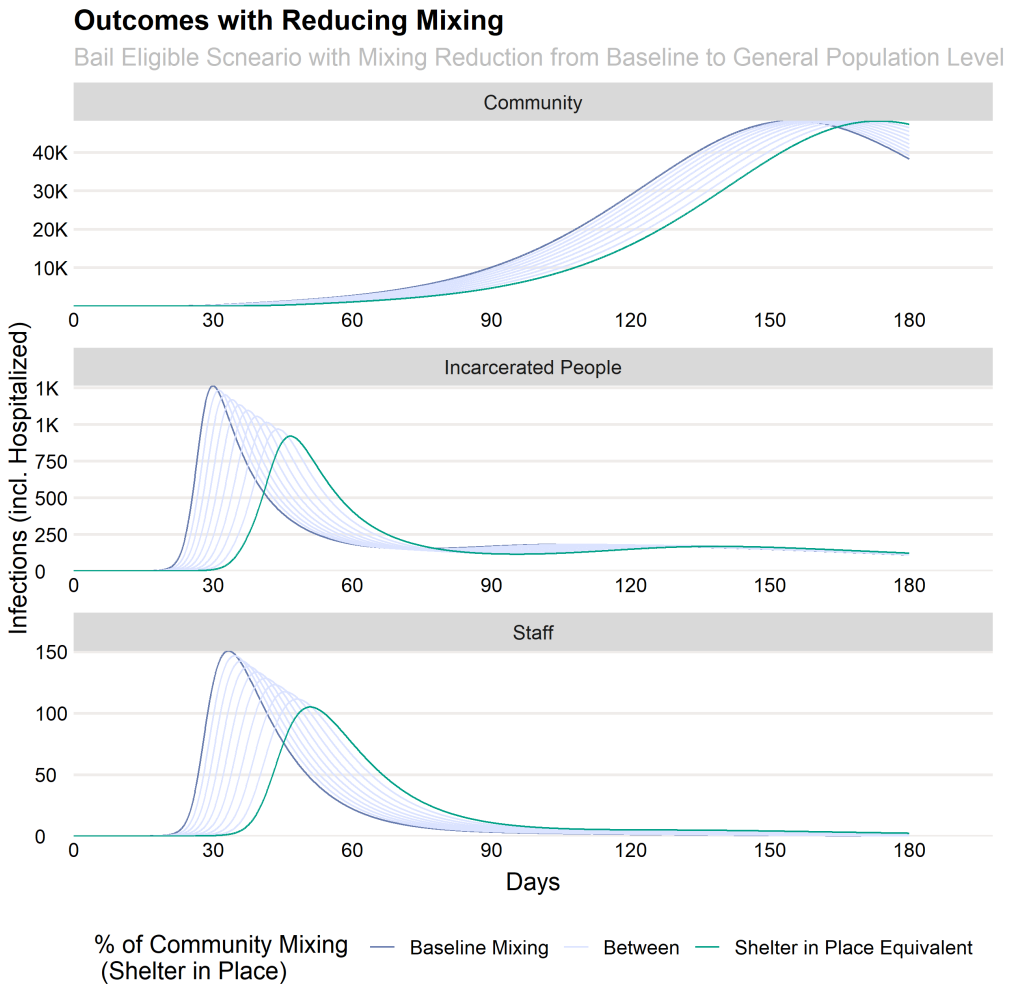

Fig 6. Epidemic curves for the community (top panel), persons in jail (middle panel) and jail staff (bottom panel) under a shelter in place order as well as the deferment of bail-eligible persons. The curves show the impact of increased reduction in mixing (e.g. from the ability to physically distance persons in jail while in common areas) from baseline (dark blue) to identical to the community's shelter-in-place order (green). This shifts the epidemic curve in the community slightly, and results in both a shifted and decreased curve among persons in jail as well as staff.

An increase in the detection of severe COVID-19 cases among incarcerated persons from 95% to 100% (equivalent to the same detection of the need for medical treatment available in the community) unsurprisingly increased the number of hospitalizations, as 5 out of every 100 incarcerated persons needing hospitalization were no longer missed, either for lack of access to care, insufficient diagnostic capacity, or other reasons. Similarly, owing to the vast reduction in the case fatality rate between hospitalized (CFR = 5% for low risk and 33.3% for high risk) severe cases and unhospitalized severe cases (CFR = 100% for both groups), the number of deaths dropped by 72.2% when the detection of severe cases rose to the same level as the community. Between these scenarios, the number of infections rose slightly with better detection, increasing by 0.08% (Fig 7). This is likely due to the slightly longer time an untreated severe case spends in the incarcerated population before they are removed due to death vs. when a treated case is transferred for hospitalization. This effect will only be present if the level

medRxiv preprint doi: https://doi.org/10.1101/2020.04.08.20058842; this version posted May 4, 2020. The copyright holder for this preprint (which was not certified by peer review) is the author/funder, who has granted medRxiv a license to display the preprint in perpetuity. It is made available under a CC-BY-NC-ND 4.0 International license .

of viral shedding is constant (or increasing) over the course of a clinical infection. If instead the mechanism by which a severe COVID-19 patient dies is a cytokine storm or other process not involving the virus overwhelming the immune system, we would not expect this effect to be observed. However, even in the pessimistic case wherein viral shedding is constant throughout the clinical course of infection, the slight rise in infections is offset by the decrease in the number of COVID-19 related fatalities.

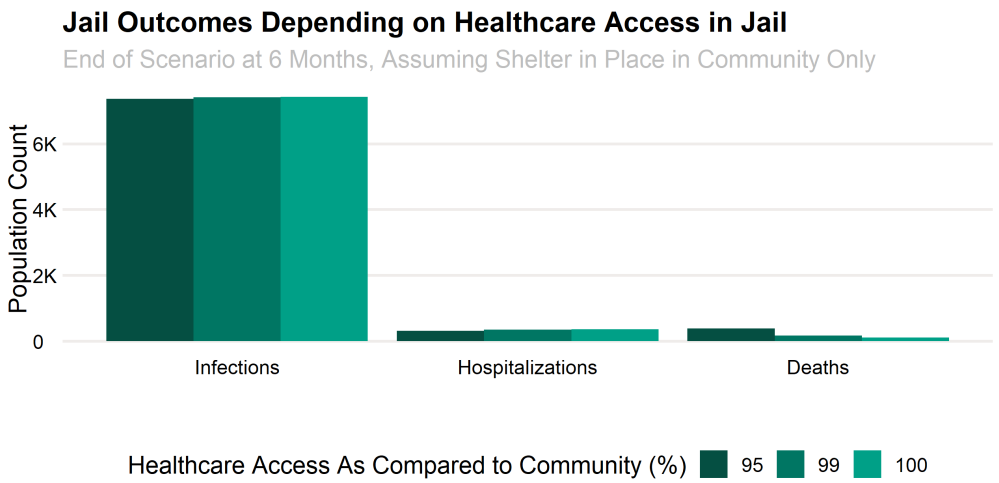

Fig 7. Infections, hospitalizations and deaths from COVID-19 among incarcerated persons under three scenarios of the probability that a severe case will be detected and receive adequate medical care. Increasing this probability results in more hospitalizations, dramatically reduced deaths, and a very slight rise in the number of infections among incarcerated persons.

Discussion

Failure to adequately protect jail populations will have a profound impact on the health of incarcerated people, corrections officers, workers in the judicial system, and members of the broader community. Our model demonstrates that, in the absence of community mitigation such as strict social distancing, by only 30 days after the introduction of the first infection to the community, we can expect 2566 infections among incarcerated people, resulting in three in-custody deaths. When contrasted with a baseline model of the general population without interaction with a jail, we see that the existence of jail-driven disease dynamics increase the total number of cases in the population by 365 and the total number of deaths by 267.

These results clearly follow from the features of the jail system themselves in challenging ways. While only 1% of the population entering into the jail system are elderly [31], incarceration in jail itself degrades the health of incarcerated people [16–18], leaving them more vulnerable to infection and severe outcomes from infection [32]. As individual robustness to disease decreases, the epidemiological result is the increased vulnerability of the whole jail population.

Beyond the direct implications for the health of incarcerated people, jail populations have high rates of re-entry into the general community and they depend on people who regularly mix with the outside community. Jail populations are largely composed of individuals who have not been convicted of a crime, and therefore will be released quickly back into the general community rather than to further incarceration within the carceral system. Jails with disease prevalence higher than the general populations they

medRxiv preprint doi: https://doi.org/10.1101/2020.04.08.20058842; this version posted May 4, 2020. The copyright holder for this preprint (which was not certified by peer review) is the author/funder, who has granted medRxiv a license to display the preprint in perpetuity. It is made available under a CC-BY-NC-ND 4.0 International license .

serve will therefore act as sources of infection, re-seeding infection into communities that may be striving to contain or mitigate ongoing outbreaks, or even reintroducing infection into otherwise disease-free populations. It is important to note that this would happen even if no one were released given the volume of people coming in and out of jails in staff and vendor roles, so should therefore not be construed as an implication that releases should be suspended or impeded.

We are not helpless to effect change. Some obvious potential courses of action suggest themselves immediately. New arrests mean that people of unknown disease status may be regularly brought into jails, increasing the likely severity of outbreaks both by the plausible continuous introduction of new sources of infection and by the maintenance of higher rates of contact among susceptible incarcerated people due to the density and structure of jail housing arrangements. If jurisdictions across the country reduce their intake by significant percentages, our models demonstrate that we will meaningfully directly reduce the disease incidence in the incarcerated population (as seen in Fig 4). Moreover, these same strategies also clearly produced a reduction in the source of risk to incarcerated people's families, jail staff, and the broader community (Fig 4). These strategies could be enacted in a number of ways, such as (but not limited to) replacing misdemeanor arrests with citations, avoiding recommendations for jail time or prohibitive terms for bail conditions, or refusing to detain anyone for nonpayment of fines or fees during the course of the outbreak.

Having considered these potential strategies for categorical reduction in intake into jails, we also considered the case in which the categorical consideration for reduction in intake stemmed instead from the health of the arrested person. In this case, we get the expected reduction in the within-jail outbreak that would have been associated with a general reduction of the same percent intake ($\approx$36.9%, allowing for a small number of incarcerations in these groups), but we fail to achieve any significant reduction in disease burden in the broader community by taking this action. It is therefore more effective to reduce the intake rate across the entire population than to attempt to single out particular categories of individuals due to their likely susceptibility to severe morbidity or mortality from infection. The larger the reduction in overall intake, the greater the reduction in disease achieved for all populations (incarcerated people, the broader community, and jail staff, in decreasing proportion of effect). These broader interventions are also likely to be relatively straightforward to implement administratively, without knowledge of an individual's underlying comorbidities, if any.

In addition to reducing rates of intake into the jail system, another obvious, concrete step we might take to reduce disease risks for everyone is to increase the rate of release from jails. This should clearly be coupled with a decreased rate of intake rather than enacted in isolation, since increasing release rates while maintaining the same rate of intake would increase infection risks for incarcerated people, the staff who work at the jails and court systems, and the broader community. This may even still occur when expedited release is coupled with decreased rates of intake if the rate of release is insufficient; see Fig 5. Again, our results clearly demonstrate that the greater the proportion of the incarcerated population we can include in such a policy, the more effective the intervention is at mitigating the outbreak.

To be maximally effective, each of these interventions should anticipate, rather than react to, widespread infection incidence in jail populations.

Critically, the factors that cause these outbreak dynamics and drive the resulting efficacy of proposed interventions are features implicit in the nature of the jail system itself. The living conditions foster disease spread. Incarcerated people are shuttled back and forth to court or, where court proceedings are halted due to this pandemic, forced to remain in their cells or dorms. Incarcerated people occupy shared spaces in which physical distancing is impossible either due to space, overcrowding, or the requirement

medRxiv preprint doi: https://doi.org/10.1101/2020.04.08.20058842; this version posted May 4, 2020. The copyright holder for this preprint (which was not certified by peer review) is the author/funder, who has granted medRxiv a license to display the preprint in perpetuity. It is made available under a CC-BY-NC-ND 4.0 International license .

of constant supervision. Incarcerated people are often not provided with the means to disinfect their surroundings or practice all of the hygiene guidelines suggested by the CDC. Improved facility sanitation, access to free personal hygienic care, such as warm water, free soap, free hand sanitizer, and free cleaning products, increased time spent outside, increased physical/social distancing measures, decreased population density achieved by releasing people, increased access to free medical care, and improved nutrition are all factors resulting in instant and obvious improvements in individual health outcomes for people incarcerated within the jail system. Alterations to function and practice of the jail system that can correct for these challenges are unlikely to occur quickly enough or substantially enough to improve the epidemiological risks for the incarcerated people within the jail system. As our results have shown, even when the within-jail transmission rates are improved by interventions such as reduction in intake from new arrests leading to a decrease in the size of the incarcerated population, we cannot effectively reduce the outbreak of infection in either the staff or incarcerated people down to the levels of the broader community.

As with all models, the conclusions of this study depend on an accurate representation of the flow of individuals between the jail system and the wider community, either due to arrests or due to their employment as jail staff, as well as the values of the parameters used to determine how swiftly this flow occurs. The inherent nature of emerging epidemics makes both of these things uncertain — the clinical and biological aspects of the pathogen might not be fully understood, and the data needed to parameterize these models is often sparse and incomplete. This problem is especially acute in models of this sort, which seek to present a "what-if" scenario to stave off a public health crisis, rather than analyze how that crisis unfolded after the fact. Nevertheless, while the exact projected magnitudes may be sensitive to these unknowns, in truth, the greatest utility of models such as these in in determining best courses of action and likely magnitudes of the effects that can be gained from those actions, rather than exact predictions of precise numbers of individuals [33]. Due to the logical nature of the processes studied, so long as errors in the parameters used are consistent across scenarios, they will not impact the understanding that results from our projections about which courses of action achieve the best outcomes, even if those errors would alter our understanding of the precise amount of effect achieved by each intervention.

Conclusion

Conditions within jails must be immediately improved to decrease the probabilities of disease transmission and support better health for incarcerated people to protect not only themselves, but also jail staff and the community at large. Decreasing population density both directly decreases disease exposure, interrupting transmission dynamics, and also facilitates many other interventions. It is a natural result of reduced intake. We can achieve/enable many desired benefits with just that one, simple action, but to achieve maximal benefits to society, preventing the greatest burden from disease both within the jails and without, broad actions that include alterations to both intake and release and also many of the within-jail strategies for improving the individual means to enact personal hygiene, protection through social distancing, and access to medical care are all needed.

Acknowledgments

EL was supported by the CDC Cooperative Agreement RFA-CK-17-001-Modeling Infectious Diseases in Healthcare Program (MInD-Healthcare).

medRxiv preprint doi: https://doi.org/10.1101/2020.04.08.20058842; this version posted May 4, 2020. The copyright holder for this preprint (which was not certified by peer review) is the author/funder, who has granted medRxiv a license to display the preprint in perpetuity. It is made available under a CC-BY-NC-ND 4.0 International license .

References

1. Mervosh S, Lu D, Swales V. See Which States and Cities Have Told Residents to Stay at Home. New York Times. 2020;.

2. Bayham J, Fenichel EP. The Impact of School Closure for COVID-19 on the US Healthcare Workforce and the Net Mortality Effects. Available at SSRN 3555259. 2020;.

3. Sharp R. The Incarceration Nation: Interpreting the United States Imprisonment Rate. 2018;.

4. Sykes BL, Pettit B. Measuring the Exposure of Parents and Children to Incarceration. In: Handbook on Children with Incarcerated Parents. Springer; 2019. p. 11–23.

5. Weidner RR, Schultz J. Examining the relationship between US incarceration rates and population health at the county level. SSM-Population Health. 2019;9:100466.

6. Kelley S. MASS INCARCERATION. Human Ecology. 2019;47(1):15–15.

7. Enns PK, Yi Y, Comfort M, Goldman AW, Lee H, Muller C, et al. What percentage of Americans have ever had a family member incarcerated?: Evidence from the family history of incarceration survey (FamHIS). Socius. 2019;5:2378023119829332.

8. Lester HD, Miller MJ. Discrete Event Simulation of Jail Operations in Pursuit of Organizational Culture Change. In: Computer Security. Springer; 2019. p. 307–322.

9. Minton TD. Jail Inmates at Midyear 2010 - Statistical Tables. Bureau of Justice Statistics. 2011;.

10. Raher S. The Company Store: A Deeper Look at Prison Commissaries; 2018. Available from: `https://www.prisonpolicy.org/reports/commissary.html`.

11. Bick JA. Infection control in jails and prisons. Clinical Infectious Diseases. 2007;45(8):1047–1055.

12. Hoge CW, Reichler MR, Dominguez EA, Bremer JC, Mastro TD, Hendricks KA, et al. An Epidemic of Pneumococcal Disease in an Overcrowded, Inadequately Ventilated Jail. New England Journal of Medicine. 1994;331(10):643–648. doi:10.1056/NEJM199409083311004.

13. Nowotny KM. Health care needs and service use among male prison inmates in the United States: A multi-level behavioral model of prison health service utilization. Health & justice. 2017;5(1):9.

14. Mignon S. Health issues of incarcerated women in the United States. Ciencia & saude coletiva. 2016;21:2051–2060.

15. Barnert ES, Perry R, Morris RE. Juvenile incarceration and health. Academic pediatrics. 2016;16(2):99–109.

16. McClelland DC, Alexander C, Marks E. The need for power, stress, immune function, and illness among male prisoners. Journal of Abnormal Psychology. 1982;91(1):61.

medRxiv preprint doi: https://doi.org/10.1101/2020.04.08.20058842; this version posted May 4, 2020. The copyright holder for this preprint (which was not certified by peer review) is the author/funder, who has granted medRxiv a license to display the preprint in perpetuity. It is made available under a CC-BY-NC-ND 4.0 International license .

17. Jacobs ET, Mullany CJ. Vitamin D deficiency and inadequacy in a correctional population. Nutrition. 2015;31(5):659–663.

18. Kouyoumdjian FG, Andreev EM, Borschmann R, Kinner SA, McConnon A. Do people who experience incarceration age more quickly? Exploratory analyses using retrospective cohort data on mortality from Ontario, Canada. PloS one. 2017;12(4).

19. Wagner P, Sakala L. Mass incarceration: The whole pie. Prison Policy Initiative. 2014;12.

20. Yuan HY, Baguelin M, Kwok KO, Arinaminpathy N, van Leeuwen E, Riley S. The impact of stratified immunity on the transmission dynamics of influenza. Epidemics. 2017;20:84–93.

21. Rohani P, Zhong X, King AA. Contact network structure explains the changing epidemiology of pertussis. Science. 2010;330(6006):982–985.

22. Ferguson N, Laydon D, Nedjati Gilani G, Imai N, Ainslie K, Baguelin M, et al. Report 9: Impact of non-pharmaceutical interventions (NPIs) to reduce COVID19 mortality and healthcare demand. 2020;.

23. Hu Z, Song C, Xu C, Jin G, Chen Y, Xu X, et al. Clinical characteristics of 24 asymptomatic infections with COVID-19 screened among close contacts in Nanjing, China. Science China Life Sciences. 2020; p. 1–6.

24. Weitz JS. COVID-19 Epidemic Risk Assessment for Georgia. Available on GitHub. 2020;.

25. Lauer SA, Grantz KH, Bi Q, Jones FK, Zheng Q, Meredith HR, et al. The incubation period of coronavirus disease 2019 (COVID-19) from publicly reported confirmed cases: estimation and application. Annals of internal medicine. 2020;.

26. Verity R, Okell LC, Dorigatti I, Winskill P, Whittaker C, Imai N, et al. Estimates of the severity of COVID-19 disease. MedRxiv. 2020;.

27. Tindale L, Coombe M, Stockdale JE, Garlock E, Lau WYV, Saraswat M, et al. Transmission interval estimates suggest pre-symptomatic spread of COVID-19. medRxiv. 2020;.

28. COVID C. Severe Outcomes Among Patients with Coronavirus Disease 2019 (COVID-19)—United States, February 12–March 16, 2020;.

29. Maruschak LM, Berzofsky M, Unangst J. Medical problems of state and federal prisoners and jail inmates, 2011-12. US Department of Justice, Office of Justice Programs, Bureau of Justice . . . ; 2015.

30. Pennsylvania A. Punishing Poverty: Cash Bail In Allegheny County; 2019. Available from: `https://aclupa.org/sites/default/files/field_documents/allegheny_county_report_final.pdf`.

31. Allegheny County Jail Population Management: Interactive Dashboards; 2020. Available from: `https://www.alleghenycountyanalytics.us/index.php/2019/11/04/allegheny-county-jail-population-management-dashboards-2/`.

medRxiv preprint doi: https://doi.org/10.1101/2020.04.08.20058842; this version posted May 4, 2020. The copyright holder for this preprint (which was not certified by peer review) is the author/funder, who has granted medRxiv a license to display the preprint in perpetuity. It is made available under a CC-BY-NC-ND 4.0 International license .

32. Binswanger IA, Blatchford PJ, Forsyth SJ, Stern MF, Kinner SA. Epidemiology of infectious disease–related death after release from prison, Washington State, United States, and Queensland, Australia: A Cohort Study. Public Health Reports. 2016;131(4):574–582.

33. Lofgren ET, Halloran ME, Rivers CM, Drake JM, Porco TC, Lewis B, et al. Opinion: Mathematical models: A key tool for outbreak response. Proceedings of the National Academy of Sciences. 2014;111(51):18095–18096.

34. Stein M. Large sample properties of simulations using Latin hypercube sampling. Technometrics. 1987;29(2):143–151.

Supporting information

SI Appendix 1. According to the logic presented in the Model/Methods section 1 define the following system of equations to capture the epidemiological dynamics of our system:

Within the Broader Community:

$$\begin{aligned}
\frac{dS_K^C}{dt} &= -\beta_{KK}^C S_K^C \left(I_K^C + \sigma E_K^C\right) - \beta_{KL}^C S_K^C \left(I_L^C + I_O^C + \sigma\left(E_L^C + E_O^C\right)\right) \\
&\quad - \beta_{KE}^C S_K^C \left(I_E^C + \sigma E_E^C\right) - \beta_{KH}^C S_K^C \left(I_H^C + \sigma E_H^C\right) \\
\frac{dE_K^C}{dt} &= \beta_{KK}^C S_K^C \left(I_K^C + \sigma E_K^C\right) + \beta_{KL}^C S_K^C \left(I_L^C + I_O^C + \sigma\left(E_L^C + E_O^C\right)\right) \\
&\quad + \beta_{KE}^C S_K^C \left(I_E^C + \sigma E_E^C\right) + \beta_{KH}^C S_K^C \left(I_H^C + \sigma E_H^C\right) - \left(\gamma + \hat{\gamma}\right) E_K^C \\
\frac{dI_K^C}{dt} &= \gamma E_K^C - \delta I_K^C \\
\frac{dR_K^C}{dt} &= \delta I_K^C + \hat{\gamma} E_K^C \\
\frac{dS_L^C}{dt} &= -\beta_{LK}^C S_L^C \left(I_K^C + \sigma E_K^C\right) - \beta_{LL}^C S_L^C \left(I_L^C + I_O^C + \sigma\left(E_L^C + E_O^C\right)\right) \\
&\quad - \beta_{LE}^C S_L^C \left(I_E^C + \sigma E_E^C\right) - \beta_{LH}^C S_L^C \left(I_H^C + \sigma E_H^C\right) - \alpha_L S_L^C + \psi_C S_L^P + \rho S_L^J \\
\frac{dE_L^C}{dt} &= \beta_{LK}^C S_L^C \left(I_K^C + \sigma E_K^C\right) + \beta_{LL}^C S_L^C \left(I_L^C + I_O^C + \sigma\left(E_L^C + E_O^C\right)\right) \\
&\quad + \beta_{LE}^C S_L^C \left(I_E^C + \sigma E_E^C\right) + \beta_{LH}^C S_L^C \left(I_H^C + \sigma E_H^C\right) - \left(\gamma + \hat{\gamma}\right) E_L^C \\
&\quad - \alpha_L E_L^C + \psi_C E_L^P + \rho E_L^J \\
\frac{dI_L^C}{dt} &= \gamma E_L^C - \delta I_L^C - \omega_L I_L^C - \alpha_L I_L^C + \psi_C I_L^P + \rho I_L^J \\
\frac{dM_L^C}{dt} &= \omega_L I_L^C - \delta_{Discharge} \nu M_L^C - \delta_{Death}(1-\nu) M_L^C \\
\frac{dR_L^C}{dt} &= \delta I_L^C + \hat{\gamma} E_L^C + \delta_{Discharge} \nu M_L^C + \delta_{Death}(1-\nu) M_L^C - \alpha_L R_L^C + \psi_C R_L^P \\
&\quad + \rho R_L^J \\
\frac{dS_E^C}{dt} &= -\beta_{EK}^C S_E^C \left(I_K^C + \sigma E_K^C\right) - \beta_{EL}^C S_E^C \left(I_L^C + I_O^C + \sigma\left(E_L^C + E_O^C\right)\right) \\
&\quad - \beta_{EE}^C S_E^C \left(I_E^C + \sigma E_E^C\right) - \beta_{EH}^C S_E^C \left(I_H^C + \sigma E_H^C\right) - \alpha_E S_E^C + \psi_C S_E^P + \rho S_E^J
\end{aligned}$$

medRxiv preprint doi: https://doi.org/10.1101/2020.04.08.20058842; this version posted May 4, 2020. The copyright holder for this preprint (which was not certified by peer review) is the author/funder, who has granted medRxiv a license to display the preprint in perpetuity. It is made available under a CC-BY-NC-ND 4.0 International license .

$$\frac{dE_E^C}{dt} = \beta_{EK}^C S_E^C \left(I_K^C + \sigma E_K^C\right) + \beta_{EL}^C S_E^C \left(I_L^C + I_O^C + \sigma\left(E_L^C + E_O^C\right)\right) + \beta_{EE}^C S_E^C \left(I_E^C + \sigma E_E^C\right) + \beta_{EH}^C S_E^C \left(I_H^C + \sigma E_H^C\right) - (\gamma + \hat{\gamma}) E_E^C - \alpha_E E_E^C + \psi_C E_E^P + \rho E_E^J$$

$$\frac{dI_E^C}{dt} = \gamma E_E^C - \delta I_E^C - \omega_H I_E^C - \alpha_E I_E^C + \psi_C I_E^P + \rho I_E^J$$

$$\frac{dM_E^C}{dt} = \omega_H I_E^C - \delta_{Discharge}\nu_H M_E^C - \delta_{Death}(1-\nu_H) M_E^C$$

$$\frac{dR_E^C}{dt} = \delta I_E^C + \hat{\gamma} E_E^C + \delta_{Discharge}\nu_H M_E^C + \delta_{Death}(1-\nu_H) M_E^C - \alpha_H R_E^C + \psi_C R_E^P + \rho R_E^J$$

$$\frac{dS_H^C}{dt} = -\beta_{HK}^C S_H^C \left(I_K^C + \sigma E_K^C\right) - \beta_{HL}^C S_H^C \left(I_L^C + I_O^C + \sigma\left(E_L^C + E_O^C\right)\right) - \beta_{HE}^C S_H^C \left(I_E^C + \sigma E_E^C\right) - \beta_{HH}^C S_H^C \left(I_H^C + \sigma E_H^C\right) - \alpha_H S_H^C + \psi_C S_H^P + \rho S_H^J$$

$$\frac{dE_H^C}{dt} = \beta_{HK}^C S_H^C \left(I_K^C + \sigma E_K^C\right) + \beta_{HL}^C S_H^C \left(I_L^C + I_O^C + \sigma\left(E_L^C + E_O^C\right)\right) + \beta_{HE}^C S_H^C \left(I_E^C + \sigma E_E^C\right) + \beta_{HH}^C S_H^C \left(I_H^C + \sigma E_H^C\right) - (\gamma + \hat{\gamma}) E_H^C - \alpha_H E_H^C + \psi_C E_H^P + \rho E_H^J$$

$$\frac{dI_H^C}{dt} = \gamma E_H^C - \delta I_H^C - \omega_H I_H^C - \alpha_H I_H^C + \psi_C I_H^P + \rho I_H^J$$

$$\frac{dM_H^C}{dt} = \omega_H I_H^C - \delta_{Discharge}\nu_H M_H^C - \delta_{Death}(1-\nu_H) M_H^C$$

$$\frac{dR_H^C}{dt} = \delta I_H^C + \hat{\gamma} E_H^C + \delta_{Discharge}\nu_H M_H^C + \delta_{Death}(1-\nu_H) M_H^C - \alpha_H R_H^C + \psi_C R_H^P + \rho R_H^J$$

$$\frac{dS_O^C}{dt} = -\beta_{OK}^C S_O^C \left(I_K^C + \sigma E_K^C\right) - \beta_{OL}^C S_O^C \left(I_L^C + I_O^C + \sigma\left(E_L^C + E_O^C\right)\right) - \beta_{OE}^C S_O^C \left(I_E^C + \sigma E_E^C\right) - \beta_{OH}^C S_O^C \left(I_H^C + \sigma E_H^C\right) - \mu_J S_O^C + \mu_C S_O^J$$

$$\frac{dE_O^C}{dt} = \beta_{OK}^C S_O^C \left(I_K^C + \sigma E_K^C\right) + \beta_{OL}^C S_O^C \left(I_L^C + I_O^C + \sigma\left(E_L^C + E_O^C\right)\right) + \beta_{OE}^C S_O^C \left(I_E^C + \sigma E_E^C\right) + \beta_{OH}^C S_O^C \left(I_H^C + \sigma E_H^C\right) - (\gamma + \hat{\gamma}) E_O^C - \mu_J E_O^C + \mu_C E_O^J$$

$$\frac{dI_O^C}{dt} = \gamma E_O^C - \delta I_O^C - \omega_L I_O^C - \mu_J I_O^C + \mu_C I_O^J$$

$$\frac{dM_O^C}{dt} = \omega_L \left(I_O^C + I_O^J\right) - \delta_{Discharge}\nu M_O^C - \delta_{Death}(1-\nu) M_O^C$$

$$\frac{dR_O^C}{dt} = \delta I_O^C + \hat{\gamma} E_O^C + \delta_{Discharge}\nu M_O^C + \delta_{Death}(1-\nu) M_O^C - \mu_J R_O^C + \mu_C R_O^J$$

Within the Processing System:

$$\frac{dS_L^P}{dt} = -\beta_{LL}^P S_L^P \left(I_L^P + I_L^T + \sigma\left(E_L^P + E_L^T\right)\right) - \beta_{LE}^P S_L^P \left(I_E^P + I_E^T + \sigma\left(E_E^P + E_E^T\right)\right) - \beta_{LH}^P S_L^P \left(I_H^P + I_H^T + \sigma\left(E_H^P + E_H^T\right)\right) + \alpha_L S_L^C - \psi_C S_L^P - \psi_J S_L^P$$

medRxiv preprint doi: https://doi.org/10.1101/2020.04.08.20058842; this version posted May 4, 2020. The copyright holder for this preprint (which was not certified by peer review) is the author/funder, who has granted medRxiv a license to display the preprint in perpetuity. It is made available under a CC-BY-NC-ND 4.0 International license .

$$\begin{aligned}
\frac{dE_L^P}{dt} &= \beta_{LL}^P S_L^P \left(I_L^P + I_L^T + \sigma\left(E_L^P + E_L^T\right)\right) + \beta_{LE}^P S_L^P \left(I_E^P + I_E^T + \sigma\left(E_E^P + E_E^T\right)\right) \\
&\quad + \beta_{LH}^P S_L^P \left(I_H^P + I_H^T + \sigma\left(E_H^P + E_H^T\right)\right) - \left(\gamma + \hat{\gamma}\right) E_L^P + \alpha_L E_L^C \\
&\quad - \ \psi_C E_L^P - \ \psi_J E_L^P \\
\frac{dI_L^P}{dt} &= \gamma E_L^P - \delta I_L^P + \alpha_L I_L^C - \ \psi_C I_L^P - \ \psi_J I_L^P \\
\frac{dR_L^P}{dt} &= \alpha_L R_L^C - \ \psi_C R_L^P - \ \psi_J R_L^P + \delta I_L^P + \hat{\gamma} E_L^P \\
\frac{dS_E^P}{dt} &= -\beta_{EL}^P S_E^P \left(I_L^P + I_L^T + \sigma\left(E_L^P + E_L^T\right)\right) - \beta_{EE}^P S_E^P \left(I_E^P + I_E^T + \sigma\left(E_E^P + E_E^T\right)\right) \\
&\quad - \beta_{EH}^P S_E^P \left(I_H^P + I_H^T + \sigma\left(E_H^P + E_H^T\right)\right) + \alpha_E S_E^C \ - \ \psi_C S_E^P - \ \psi_J S_E^P \\
\frac{dE_E^P}{dt} &= \beta_{EL}^P S_E^P \left(I_L^P + I_L^T + \sigma\left(E_L^P + E_L^T\right)\right) + \beta_{EE}^P S_E^P \left(I_E^P + I_E^T + \sigma\left(E_E^P + E_E^T\right)\right) \\
&\quad + \beta_{EH}^P S_E^P \left(I_H^P + I_H^T + \sigma\left(E_H^P + E_H^T\right)\right) - \left(\gamma + \hat{\gamma}\right) E_E^P + \alpha_E E_E^C \\
&\quad - \ \psi_C E_E^P - \ \psi_J E_E^P \\
\frac{dI_E^P}{dt} &= \gamma E_E^P - \delta I_E^P + \alpha_E I_E^C - \ \psi_C I_E^P - \ \psi_J I_E^P \\
\frac{dR_E^P}{dt} &= \alpha_E R_E^C - \ \psi_C R_E^P - \ \psi_J R_E^P + \delta I_E^P + \hat{\gamma} E_E^P \\
\frac{dS_H^P}{dt} &= -\beta_{HL}^P S_H^P \left(I_L^P + I_L^T + \sigma\left(E_L^P + E_L^T\right)\right) - \beta_{HE}^P S_H^P \left(I_E^P + I_E^T + \sigma\left(E_E^P + E_E^T\right)\right) \\
&\quad - \beta_{HH}^P S_H^P \left(I_H^P + I_H^T + \sigma\left(E_H^P + E_H^T\right)\right) + \alpha_H S_H^C - \ \psi_C S_H^P - \ \psi_J S_H^P \\
\frac{dE_H^P}{dt} &= \beta_{HL}^P S_H^P \left(I_L^P + I_L^T + \sigma\left(E_L^P + E_L^T\right)\right) + \beta_{HE}^P S_H^P \left(I_E^P + I_E^T + \sigma\left(E_E^P + E_E^T\right)\right) \\
&\quad + \beta_{HH}^P S_H^P \left(I_H^P + I_H^T + \sigma\left(E_H^P + E_H^T\right)\right) - \left(\gamma + \hat{\gamma}\right) E_H^P + \alpha_H E_H^C \\
&\quad - \ \psi_C E_H^P - \ \psi_J E_H^P \\
\frac{dI_H^P}{dt} &= \gamma E_H^P - \delta I_H^P + \alpha_H I_H^C - \ \psi_C I_H^P - \ \psi_J I_H^P \\
\frac{dR_H^P}{dt} &= \alpha_H R_H^C - \ \psi_C R_H^P - \ \psi_J R_H^P + \delta I_H^P + \hat{\gamma} E_H^P
\end{aligned}$$

Within the Trial System:

$$\begin{aligned}
\frac{dS_L^T}{dt} &= -\beta_{LL}^T S_L^T \left(I_L^P + I_L^T + \sigma\left(E_L^P + E_L^T\right)\right) - \beta_{LE}^T S_L^T \left(I_E^P + I_E^T + \sigma\left(E_E^P + E_E^T\right)\right) \\
&\quad - \beta_{LH}^T S_L^T \left(I_H^P + I_H^T + \sigma\left(E_H^P + E_H^T\right)\right) + \ \kappa\tau S_L^J \ - \kappa S_L^T \\
\frac{dE_L^T}{dt} &= \beta_{LL}^T S_L^T \left(I_L^P + I_L^T + \sigma\left(E_L^P + E_L^T\right)\right) + \beta_{LE}^T S_L^T \left(I_E^P + I_E^T + \sigma\left(E_E^P + E_E^T\right)\right) \\
&\quad + \beta_{LH}^T S_L^T \left(I_H^P + I_H^T + \sigma\left(E_H^P + E_H^T\right)\right) - \left(\gamma + \hat{\gamma}\right) E_L^T + \ \kappa\tau E_L^J - \kappa E_L^T \\
\frac{dI_L^T}{dt} &= \gamma E_L^T - \delta I_L^T + \ \kappa\tau I_L^J - \kappa I_L^T \\
\frac{dR_L^T}{dt} &= \kappa\tau R_L^J - \kappa R_L^T + \delta I_L^T + \hat{\gamma} E_L^T
\end{aligned}$$

medRxiv preprint doi: https://doi.org/10.1101/2020.04.08.20058842; this version posted May 4, 2020. The copyright holder for this preprint (which was not certified by peer review) is the author/funder, who has granted medRxiv a license to display the preprint in perpetuity. It is made available under a CC-BY-NC-ND 4.0 International license .

$$
\begin{aligned}
\frac{dS_E^T}{dt} &= -\beta_{EL}^T S_E^T \left(I_L^P + I_L^T + \sigma\left(E_L^P + E_L^T\right)\right) - \beta_{EE}^T S_E^T \left(I_E^P + I_E^T + \sigma\left(E_E^P + E_E^T\right)\right) \\
&\quad - \beta_{EH}^T S_E^T \left(I_H^P + I_H^T + \sigma\left(E_H^P + E_H^T\right)\right) + \ \kappa\tau S_E^J \ - \kappa S_E^T \\
\frac{dE_E^T}{dt} &= \beta_{EL}^T S_E^T \left(I_L^P + I_L^T + \sigma\left(E_L^P + E_L^T\right)\right) + \beta_{EE}^T S_E^T \left(I_E^P + I_E^T + \sigma\left(E_E^P + E_E^T\right)\right) \\
&\quad + \beta_{EH}^T S_E^T \left(I_H^P + I_H^T + \sigma\left(E_H^P + E_H^T\right)\right) - \left(\gamma + \hat{\gamma}\right) E_E^T + \ \kappa\tau E_E^J - \kappa E_E^T \\
\frac{dI_E^T}{dt} &= \gamma E_E^T - \delta I_E^T + \ \kappa\tau I_E^J - \kappa I_E^T \\
\frac{dR_E^T}{dt} &= \kappa\tau R_E^J - \kappa R_E^T + \delta I_E^T + \hat{\gamma} E_E^T \\
\frac{dS_H^T}{dt} &= -\beta_{HL}^T S_H^T \left(I_L^P + I_L^T + \sigma\left(E_L^P + E_L^T\right)\right) - \beta_{HE}^T S_H^T \left(I_E^P + I_E^T + \sigma\left(E_E^P + E_E^T\right)\right) \\
&\quad - \beta_{HH}^T S_H^T \left(I_H^P + I_H^T + \sigma\left(E_H^P + E_H^T\right)\right) + \kappa\tau S_H^J - \kappa S_H^T \\
\frac{dE_H^T}{dt} &= \beta_{HL}^T S_H^T \left(I_L^P + I_L^T + \sigma\left(E_L^P + E_L^T\right)\right) + \beta_{HE}^T S_H^T \left(I_E^P + I_E^T + \sigma\left(E_E^P + E_E^T\right)\right) \\
&\quad + \beta_{HH}^T S_H^T \left(I_H^P + I_H^T + \sigma\left(E_H^P + E_H^T\right)\right) - \left(\gamma + \hat{\gamma}\right) E_H^T + \kappa\tau E_H^J - \kappa E_H^T \\
\frac{dI_H^T}{dt} &= \gamma E_H^T - \delta I_H^T + \kappa\tau I_H^J - \kappa I_H^T \\
\frac{dR_H^T}{dt} &= \kappa\tau R_H^J - \kappa R_H^T \ + \ \delta I_H^T + \hat{\gamma} E_H^T
\end{aligned}
$$

Within the Jail System:

$$
\begin{aligned}
\frac{dS_L^J}{dt} &= -\beta_{LL}^J S_L^J \left(I_L^J + \sigma E_L^J\right) - \beta_{LE}^J S_L^J \left(I_E^J + \sigma E_E^J\right) - \beta_{LH}^J S_L^J \left(I_H^J + \sigma E_H^J\right) \\
&\quad - \beta_{LO}^J S_L^J \left(I_O^J + \sigma E_O^J\right) + \ \psi_J S_L^P - \ \kappa\tau S_L^J - \ \rho S_L^J + \kappa S_L^T \\
\frac{dE_L^J}{dt} &= \beta_{LL}^J S_L^J \left(I_L^J + \sigma E_L^J\right) + \beta_{LE}^J S_L^J \left(I_E^J + \sigma E_E^J\right) + \beta_{LH}^J S_L^J \left(I_H^J + \sigma E_H^J\right) \\
&\quad + \beta_{LO}^J S_L^J \left(I_O^J + \sigma E_O^J\right) - \left(\gamma + \hat{\gamma}\right) E_L^J + \ \psi_J E_L^P - \ \kappa\tau E_L^J - \ \rho E_L^J + \kappa E_L^T \\
\frac{dI_L^J}{dt} &= \gamma E_L^J - \delta I_L^J - \omega_L \zeta I_L^J - \left(1 - \nu_U\right)\left(1 - \zeta\right) \delta_{Death_U} I_L^J - \nu_U \left(1 - \zeta\right) \delta_{Discharge} I_L^J \\
&\quad + \psi_J I_L^P - \ \kappa\tau I_L^J - \ \rho I_L^J + \kappa I_L^T \\
\frac{dM_L^J}{dt} &= \omega_L \zeta I_L^J - \delta_{Discharge} \nu M_L^J - \delta_{Death}(1 - \nu) M_L^J \\
\frac{dR_L^J}{dt} &= \delta I_L^J + \hat{\gamma} E_L^J + \delta_{Discharge} \nu M_L^J + \delta_{Death}(1 - \nu) M_L^J + \delta_{Death_U}(1 - \nu_U)(1 - \zeta) I_L^J \\
&\quad + \delta_{Discharge} \nu_U \left(1 - \zeta\right) I_L^J + \ \psi_J R_L^P - \ \kappa\tau R_L^J - \ \rho R_L^J + \kappa R_L^T \\
\frac{dS_E^J}{dt} &= -\beta_{EL}^J S_E^J \left(I_L^J + \sigma E_L^J\right) - \beta_{EE}^J S_E^J \left(I_E^J + \sigma E_E^J\right) - \beta_{EH}^J S_E^J \left(I_H^J + \sigma E_H^J\right) \\
&\quad - \beta_{EO}^J S_E^J \left(I_O^J + \sigma E_O^J\right) + \ \psi_J S_E^P - \ \kappa\tau S_E^J - \ \rho S_E^J + \kappa S_E^T \\
\frac{dE_E^J}{dt} &= \beta_{EL}^J S_E^J \left(I_L^J + \sigma E_L^J\right) + \beta_{EE}^J S_E^J \left(I_E^J + \sigma E_E^J\right) + \beta_{EH}^J S_E^J \left(I_H^J + \sigma E_H^J\right) \\
&\quad + \beta_{EO}^J S_E^J \left(I_O^J + \sigma E_O^J\right) - \left(\gamma + \hat{\gamma}\right) E_E^J + \ \psi_J E_E^P - \ \kappa\tau E_E^J - \ \rho E_E^J + \kappa E_E^T
\end{aligned}
$$

medRxiv preprint doi: https://doi.org/10.1101/2020.04.08.20058842; this version posted May 4, 2020. The copyright holder for this preprint (which was not certified by peer review) is the author/funder, who has granted medRxiv a license to display the preprint in perpetuity. It is made available under a CC-BY-NC-ND 4.0 International license .

$$
\begin{aligned}
\frac{dI_E^J}{dt} &= \gamma E_E^J - \delta I_E^J - \omega_H \zeta I_E^J - (1-\nu_{UH})(1-\zeta)\,\delta_{Death_U} I_E^J \\
&\quad - \nu_{UH}(1-\zeta)\,\delta_{Discharge} I_E^J + \psi_J I_E^P - \kappa\tau I_E^J - \rho I_E^J + \kappa I_E^T \\
\frac{dM_E^J}{dt} &= \omega_H \zeta I_E^J - \delta_{Discharge}\nu_H M_E^J - \delta_{Death}(1-\nu_H) M_E^J \\
\frac{dR_E^J}{dt} &= \delta I_E^J + \hat{\gamma} E_E^J + \delta_{Discharge}\nu_H M_E^J + \delta_{Death}(1-\nu_H) M_E^J \\
&\quad + \delta_{Death_U}(1-\nu_{UH})(1-\zeta) I_E^J + \delta_{Discharge}\nu_{UH}(1-\zeta)\, I_E^J + \psi_J R_E^P \\
&\quad - \kappa\tau R_E^J - \rho R_E^J + \kappa R_E^T \\
\frac{dS_H^J}{dt} &= -\beta_{HL}^J S_H^J \left(I_L^J + \sigma E_L^J\right) - \beta_{HE}^J S_H^J \left(I_E^J + \sigma E_E^J\right) - \beta_{HH}^J S_H^J \left(I_H^J + \sigma E_H^J\right) \\
&\quad - \beta_{HO}^J S_H^J \left(I_O^J + \sigma E_O^J\right) + \psi_J S_H^P - \kappa\tau S_H^J - \rho S_H^J + \kappa S_H^T \\
\frac{dE_H^J}{dt} &= \beta_{HL}^J S_H^J \left(I_L^J + \sigma E_L^J\right) + \beta_{HE}^J S_H^J \left(I_E^J + \sigma E_E^J\right) + \beta_{HH}^J S_H^J \left(I_H^J + \sigma E_H^J\right) \\
&\quad + \beta_{HO}^J S_H^J \left(I_O^J + \sigma E_O^J\right) - (\gamma + \hat{\gamma})\, E_H^J + \psi_J E_H^P - \kappa\tau E_H^J - \rho E_H^J + \kappa E_H^T \\
\frac{dI_H^J}{dt} &= \gamma E_H^J - \delta I_H^J - \omega_H \zeta I_H^J - (1-\nu_{UH})(1-\zeta)\,\delta_{Death_U} I_H^J - \nu_{UH}(1-\zeta)\,\delta_{Discharge} I_H^J \\
&\quad + \psi_J I_H^P - \kappa\tau I_H^J - \rho I_H^J + \kappa I_H^T \\
\frac{dM_H^J}{dt} &= \omega_H \zeta I_H^J - \delta_{Discharge}\nu_H M_H^J - \delta_{Death}(1-\nu_H) M_H^J \\
\frac{dR_H^J}{dt} &= \delta I_H^J + \hat{\gamma} E_H^J + \delta_{Discharge}\nu_H M_H^J + \delta_{Death}(1-\nu_H) M_H^J \\
&\quad + \delta_{Death_U}(1-\nu_{UH})(1-\zeta)\, I_H^J + \nu_{UH}(1-\zeta)\,\delta_{Discharge} I_H^J + \psi_J R_H^P \\
&\quad - \kappa\tau R_H^J - \rho R_H^J + \kappa R_H^T \\
\frac{dS_O^J}{dt} &= -\beta_{OL}^J S_O^J \left(I_L^J + I_E^J + I_H^J + \sigma\left(E_L^J + E_E^J + E_H^J\right)\right) - \beta_{OO}^J S_O^J \left(I_O^J + \sigma E_O^J\right) + \mu_J S_O^C \\
&\quad - \mu_C S_O^J \\
\frac{dE_O^J}{dt} &= \beta_{OL}^J S_O^J \left(I_L^J + I_E^J + I_H^J + \sigma\left(E_L^J + E_E^J + E_H^J\right)\right) + \beta_{OO}^J S_O^J \left(I_O^J + \sigma E_O^J\right) \\
&\quad + \mu_J E_O^C - \mu_C E_O^J - (\gamma + \hat{\gamma})\, E_O^J \\
\frac{dI_O^J}{dt} &= \mu_J I_O^C - \mu_C I_O^J + \gamma E_O^J - \delta I_O^J - \omega_L I_O^J \\
\frac{dR_O^J}{dt} &= \mu_J R_O^C - \mu_C R_O^J + \delta I_O^J + \hat{\gamma} E_O^J
\end{aligned}
$$

SI Appendix 2. The exponential survival model fit to Hu et al., 2020 estimated a mean asymptomatic shedding period of 11.79 days (95% CI: 7.86, 18.61), which is indeed a higher estimate than that found in the original manuscript, which did not account for censoring. As 5.1 of those days are already accounted for in the original estimate for $\gamma^{-}1$, this yielded an estimate for $\hat{\gamma}^{-1}$ of 6.7 days. Compared to a Kaplan-Meier fit of the available data, the exponential model fit well, and adequately models underlying survival function (Fig 8).

medRxiv preprint doi: https://doi.org/10.1101/2020.04.08.20058842; this version posted May 4, 2020. The copyright holder for this preprint (which was not certified by peer review) is the author/funder, who has granted medRxiv a license to display the preprint in perpetuity. It is made available under a CC-BY-NC-ND 4.0 International license .

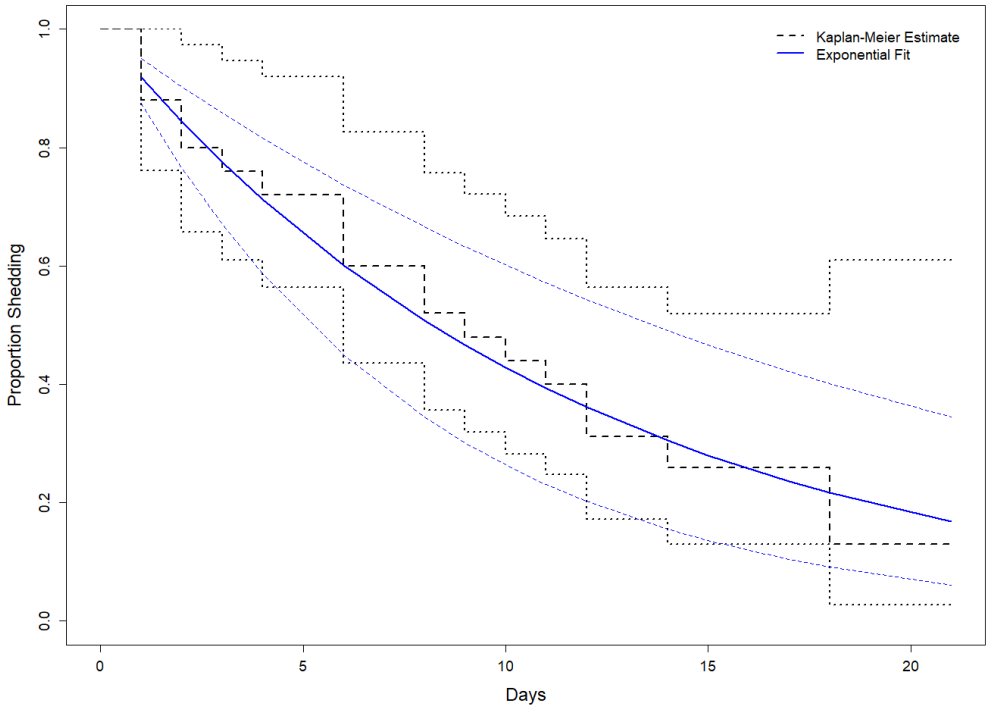

Fig 8. Proportion of patients with viral shedding among a cohort of asymptomatic COVID-19 patients in China. Original data from Hu et al., 2020. Dashed black line depicts a non-parameteric Kaplan-Meier fit, while the solid blue line depicts the fit of an exponential survival function.

medRxiv preprint doi: https://doi.org/10.1101/2020.04.08.20058842; this version posted May 4, 2020. The copyright holder for this preprint (which was not certified by peer review) is the author/funder, who has granted medRxiv a license to display the preprint in perpetuity. It is made available under a CC-BY-NC-ND 4.0 International license .

SI Appendix 3. In order to determine model sensitivity to parameter values that could not be estimated directly from published/reported data, we performed a Latin hypercube sensitivity analysis [34]. We arbitrarily selected the range of the values sampled for each parameter to be $[0.9X, 1.1X]$ where X the value reported for that parameter in Tables 1 and 2. Unsurprisingly, as with most epidemic models, this model is most sensitive to parameters that govern the duration and intensity of infectivity (i.e. σ, γ & $\hat{\gamma}$ and δ). The model was also relatively insensitive to changes in the assumed increased rates of mixing among incarcerated persons in either jail or processing, suggesting that so long as there is an increase in mixing between incarcerated persons due to the structure of jails there will remain the risk of an infectious disease outbreak, rather than this being a feature of a particular combination of parameter values.

	I_{Com}	I_{Inc}	I_{Sta}
σ	0.347336	−0.456785	−0.0004290
γ	0.469421	0.587536	0.735222
$\hat{\gamma}$	−0.595468	−0.350117	−0.735132
ω	−0.105962	−0.004185	−0.0009146
ω_H	0.0352838	−0.059627	−0.0012778
δ	−0.600617	0.607748	0.0035495
$\delta_{Discharge}$	0.0495378	−0.0692823	0.0007294
δ_{Death}	0.0487173	−0.0709513	−0.00146202
δ_{DeathU}	0.0473402	−0.0711741	−0.00243121
ν	0.0494655	−0.0686944	0.00136101
ν_H	0.0450316	−0.072549	−0.00471153
c_J	0.0594902	0.094403	0.00545029
c_P	0.053514	−0.0617216	−0.00146722

Table 4. The sensitivity of total infections (in the Community, I_{Com}, in Incarcerated People, I_{Inc}, or in the Jail Staff, I_{Sta}) after 180 days in the "Shelter in Place" scenario to perturbation of each of the parameters. For completeness, these calculations include all individuals who are ever asymptomatically infected, even if they never progress to symptomatic infection.